ISSN1027-5495. Functional Materials, 31, No.1 (2024), p. 9-12
doi:http://dx.doi.org/10.15407/fm31.01.9

Pulse-shape discrimination capability of organic composite scintillators with different grain size

I. Khromiuk, V. Alekseev, A. Krech, Ye. Martynenko, S. Minenko, O. Tarasenko

Institute for Scintillation Materials of National Academy of Sciences of Ukraine,
60 Nauky Ave., 61001 Kharkiv, Ukraine

Received November 11, 2023

The study of the pulse shape discrimination (PSD) capability for organic composite scintillators with a diameter of 20 mm and a thickness of 5 mm was carried out. The fractions of grains 0.1–0.3, 0.3–0.5, 0.5–1.0, 1.0–1.5, 1.5–2.0, 2.0–2.5 mm of *trans*-stilbene and *p*-terphenyl were used to obtain the samples. It was shown that these objects retain the dependence of their scintillation properties, namely, the figure-of-merit (FOM) value for stilbene is higher than for *p*-terphenyl. Also the composite scintillators show themselves as promising detectors, since their PSD capability is not critically lower than that of single crystal of appropriate scintillators. For the first time it was shown that for the fractions of grains under investigation, the FOM values practically do not change with increasing grain size, which indicates the same processes of transport and recombination of triplet excitons in them.

Keywords: organic composite scintillators, triplet excitons, pulse shape discrimination, figure-of-merit.

Можливість розрізнення форми імпульсу органічних композитних сцинтиляторів з різним розміром зерна. *І. Хром'юк, В. Алексєєв, А. Креч, Є. Мартиненко, С. Міненко, О. Тарасенко*

Проведено дослідження розрізнення форми імпульсу органічних композиційних сцинтиляторів діаметром 20 мм і товщиною 5 мм. Було використано фракції зерен 0,1–0,3, 0,3–0,5, 0,5–1,0, 1,0–1,5, 1,5–2,0, 2,0–2,5 мм органічних сцинтиляторів стильбену та *n*-терфенілу. Показано, що ці об'єкти зберігають залежність своїх сцинтиляційних властивостей, а саме значення FOM для стильбену вище, ніж для *n*-терфенілу, а також, що композиційні сцинтилятори є перспективними детекторами, оскільки для них ці значення є не критично нижчими, ніж у монокристалів. При цьому вперше показано, що для таких фракцій зерен значення FOM майже не відрізняється зі збільшенням розміру зерна, що свідчить про однакові процеси транспорту та рекомбінації триплетних екситонів у них.

1. Introduction

An important question is the ability of scintillation detectors to separate radiation signals with different specific energy losses (dE/dx). The importance of this issue lies in the fact that the effects of various ionizing radiations on living organisms are different. The numerical definition of this influence is the weight factor. For gamma radiation of all energies it is equal to 1, whereas for fast neutrons (energy up to 2 MeV) and alpha particles, the weight factor is 20 [1].

In organic scintillators, the ionizing radiation generates the following types of luminescent response. The ionizing radiations with large dE/dx values (recoil nuclei, alpha parti-

cles, neutrons, low-energy electrons) generate scintillation pulses with a significant part of the slow component in such systems, while radiations with low *dE*/*dx* (electrons of medium and high energies, gamma photons) give a significantly less contribution of the slow component.

There are many works devoted to the study of pulse shape discrimination (PSD) capability of organic single crystals, plastic and liquid scintillation materials (see, for example, [2–7]). In [8–10], it was shown that composite detectors (based on organic crystalline grains), like single crystals, have a high PSD capability. In [10], for the case when a ^{239}Pu-Be source irradiates samples of organic detectors, it was shown that for a reference stilbene single crystal (diameter D = 30 mm, height h = 10 mm) with the experimental setup with an energy threshold for neutron detection of 1 MeV, the FOM-value is 2.41±0.21. At the same time, for the stilbene composite detector with D = 50 mm and h = 25 mm, the FOM value was 1.89 ± 0.13, and for the stilbene composite detector with D = 50 mm and h = 50 mm, the FOM-value was 1.38 ± 0.09. Thus, the FOM-values obtained for thin composite scintillators were slightly lower than the FOM for stilbene single crystals. For thicker composite scintillators, the FOM value decreases due to lower light yield caused by greater light absorption within the scintillator. In [9], the PSD capability was studied for the case of irradiation with fast neutrons of a ^{252}Cf source. The FOM value of the stilbene composite scintillator (D = 50 mm and h = 10 mm) was estimated as 80% compared to the stilbene single crystal (D = 25 mm and h = 20 mm). The FOM-value for the large area stilbene composite scintillator (D = 200 mm and h = 20 mm) was approximately 75% compared to the stilbene single crystal (D = 50 mm and h = 40 mm). Our previous studies also confirmed this fact [11]. These results justify the need for a more in-depth study of such heterostructured scintillators.

2. Experimental

Previously, we have proposed two methods for quickly assessing the PSD capability of organic scintillators [11]. The first method of separating the radioluminescence kinetics curve obtained by the single-photon method involves searching for the zero-crossing of the second derivative of this curve. This point is further defined as the boundary between the fast and slow components, and the areas under them (S_1 for fast component and S_2 for slow component) are compared. The area ratio $r_1 = S_2/S_1$ for different ionizing radiations allows the pulse shape capability to be assessed. In the second, more accurate method, the fast component is approximated as a convolution of the exponents of the rise and decay fronts

$$N(t)\big|_{t<t_k} \sim N_0 \left\{ \exp\left(-\frac{t}{\tau_2}\right) - \exp\left(-\frac{t}{\tau_1}\right) \right\}, \quad (1)$$

where the first exponent describes the rise of the fast component with time constant t_1, and the second exponent describes the decay of the fast component with time constant t_2. The time parameter t_k was determined in turn by a linear approximation of the initial decay section of the experimental curve, using the least squares method, as a limiting value that satisfies the straight line equation $\ln(N(t))=a + bt$.

Next, the curve of the approximated fast component is subtracted from the experimental curve, and their difference is taken as the slow component. Thus, using this technique, the ratio of the slow component to the fast component ρ_2 can be obtained as the ratio of the areas under the calculated curve of the slow component S_2 and under the curve of the approximated fast component S_1:

$$\rho_2 = S_2/S_1 \quad (2)$$

Thus, the value $\zeta_{n,\gamma}$ characterizes the scintillator PSD capability:

$$\zeta_{n,\gamma} = \rho_n / \rho_\gamma . \quad (3)$$

This method was used to calculate the values shown in Table 1.

In this paper, FOM is determined by the Charge Comparison Method [12, 13]. In this method, the experimental pulse curve from an ionizing radiation is divided into certain sections relative to its maximum. The ends of these sections are predetermined for various substances and are set before starting pulse analysis. The slow (tail) part of the curve, which is identified with the slow component, is subtracted from the total curve. These ratios are collected in a histogram of the frequency of occurrence of such ratios, and following analysis of this histogram by two Gaussian curves, for the case of two excitations with different *dE*/*dx*, allows us to obtain the numerical value of FOM using the generally accepted formula:

$$FOM = \Delta S / (FWHM_1 + FWHM_2), \quad (4)$$

Table 1. The $\zeta_{n,\gamma}$-values (3)

Scintillator	$\zeta_{n,\gamma}$
Stilbene single crystal (D = 25 mm, h = 20 mm)	2.07
Stilbene composite detector (30 mm×30 mm×20 mm)	2.21
p-Terphenyl single crystal (28 mm×18 mm×18 mm)	1.31
p-Terphenyl composite detector (30 mm×30 mm×20 mm)	1.33

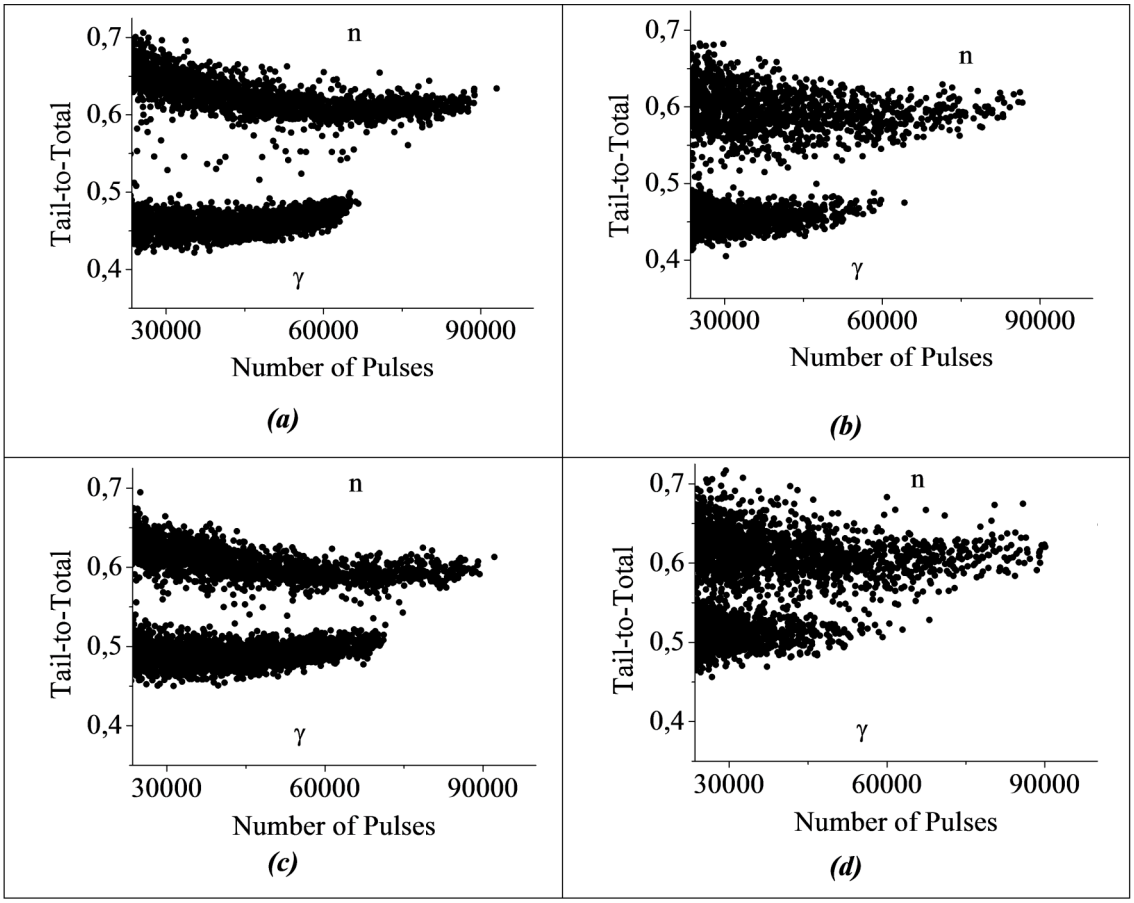

Fig. 1. Samples of PSD patterns obtained using the Charge Comparison Method: (*a*) stilbene single crystal, (*b*) composite scintillator based on stilbene grains of fraction 0.1-0.3 mm, (*c*) *p*-terphenyl single crystal, and (*d*) *p*-terphenyl composite scintillator based on stilbene grains of fraction 0.1-0.3 mm.

where ΔS is the difference in the positions of the maxima, $FWHM_1$ and $FWHM_2$ are the FWHM of the gamma and neutron peaks, respectively.

3. Results and discussion

In [11], the PSD capability $\zeta_{n,\gamma}$ (3) of stilbene and *p*-terphenyl single crystals and composite scintillators (based on a grain fraction of 1.7-2.2 mm, which was considered optimal) was assessed using the radioluminescence kinetics curves obtained by the single-photon method. We provide this information for reference.

In this work, PSD capability was studied in a more traditional way: FOM values were calculated for a similar type of scintillator, with different grain sizes from 100 μm to 2.5 mm. However, there is an important difference in their geometric sizes: the thickness of the samples in this study was only 5 mm. The diameter of single crystals was 30 mm, and that of composite scintillators was 20 mm. In Figures 1(a)–(d), as an example, we present typical sets of experimental data for stilbene and *p*-terphenyl single crystals and composite scintillators on their base with the grain fraction of 0.1–0.3 mm.

The same data were obtained for larger fractions (0.3–0.5, 0.5–1.0, 1.0–1.5, 1.5–2.0, 2.0–2.5 mm) of stilbene and *p*-terphenyl composite scintillators. Processed results are shown in Table 2 and Table 3.

Table 2. FOM values for single-crystalline and composite scintillators based on stilbene

Grain fraction, mm	FOM-value
Single crystal	2.10
0.1–0.3	1.53
0.3–0.5	1.65
0.5–1.0	1.58
1.0–1.5	1.53
1.5–2.0	1.73
2.0–2.5	1.65

Table 3. FOM values for single-crystalline and composite scintillators based on *p*-terphenyl

Grain fraction, mm	FOM-value
Single crystal	1.45
0.1–0.3	1.03
0.3–0.5	0.84
0.5–1.0	1.11
1.0–1.5	1.07
1.5–2.0	1.08
2.0–2.5	1.01

As we can see, interesting information was obtained: such small grains are still as capable of PSD as classical grains (1.7-2.2 mm), which means that all grains obtained during the preparation of grains to produce composite scintillators are still suitable for PSD due to the same physical mechanisms occurring in them.

4. Conclusions

In this work, the following results were obtained:

– for the first time, using the assessment of FOM-values, a study of the PSD capability of composite samples was carried out for a series of grain fractions, starting from 100 μm,;

– it was shown that for such grain sizes there is a tendency for stilbene-based scintillators to have a slightly better PSD capability than *p*-terphenyl-based scintillators, which was obtained in previous works by direct analysis of radioluminescence kinetics curves;

– at the same time, such ultra-fine grains still have a fairly high PSD capability.

Acknowledgements: This work was supported by the National Research Foundation of Ukraine (project No. 2021.01/0042, "Development of effective detection systems for the most harmful ionizing radiation for humans, for radioecology tasks").

References

1. ICRP Publication 103, The 2007 Recommendations of the international commission on radiological protection, Ann. ICRP, **37**, 332 (2007).
2. Birks J.B. The theory and practice of scintillation counting, London: Pergamon press, 1967; 662 p.
3. P.N. Zhmurin, V.N. Lebedev, V.D. Titskaya et al., *Nucl. Instrum. Meth. A.*, **761**, 92 (2014). https://doi.org/10.1016/j.nima.2014.05.084.
4. G. Hull, N.P. Zaitseva, N.J. Cherepy et al., *IEEE T. Nucl. Sci.*, **56**, 899 (2009). https://doi.org/10.1109/TNS.2009.2015944.
5. N.P. Zaitseva, A.M. Glenn, A.N. Mabe et al., *Nucl. Instrum. Meth. A*, **889**, 97 (2018). https://doi.org/10.1016/j.nima.2018.01.093.
6. F.D. Brooks, *Nucl. Instrum. Meth.*, **162**, 477 (1979). https://doi.org/10.1016/0029-554X(79)90729-8.
7. T. Yanagida, K. Watanabe, Y. Fujimoto, *Nucl. Instrum. Meth.*, **784**, 111 (2015). https://doi.org/10.1016/j.nima.2014.12.031.
8. S.K. Lee, Y. H. Cho, B. H. Kang et al., *J. Nucl. Sci. Technol.*, **1**, 292 (2011). http://dx.doi.org/10.15669/pnst.1.292.
9. S.K. Lee, J.B. Son, K.H. Jo et al., *J. Nucl. Sci. Technol.*, **51**, 37 (2014). http://dx.doi.org /10.1080/00223131.2014.845539.
10. J. Iwanowska, L. Swiderski, M. Moszynski et al., *J. Instrum.*, **6**, P07007 (2011). https://doi.org/10.1088/1748-0221/6/07/P07007.
11. N.Z. Galunov, I.F. Khromiuk, O.A. Tarasenko, *Nucl. Instrum. Meth. A*, **949**, 162870 (2020). https://doi.org/10.1016/j.nima.2019.162870.
12. F.D. Brooks, *Nucl. Instrum. Meth.* **162**, 477 (1979). https://doi.org/10.1016/0029-554X(79)90729-8.
13. M. Flaska, S.A. Pozzi. *Nucl. Instr. Meth. A,* **577**, 654–663 (2007). https://doi.org/10.1016/j.nima.2007.04.141